THE JOURNAL OF PHYSICAL CHEMISTRY Letters

LETTER

pubs.acs.org/JPCL

Magnetic Field Control of the Current through Molecular Ring Junctions

Dhurba Rai, Oded Hod,* and Abraham Nitzan

School of Chemistry, Tel Aviv University, Tel Aviv 69978, Israel

ABSTRACT: Whereas conducting loops are, in principle, sensitive to external magnetic field, as is pronouncedly exemplified by the Aharonov−Bohm (AB) effect, the small radius of molecular rings makes the observation of such effects challenging. Indeed, the unrealistically large magnetic field needed to realize the AB effect in molecular rings has led to a widespread belief that molecular conduction is insensitive to laboratory realizable fields. Here we revisit this issue, presenting conditions under which magnetic field control of molecular ring conduction is realizable with pronounced effects on the $I-V$ characteristics. We find these conditions to be (a) weak molecule-lead coupling, implying relatively distinct conduction resonances, (b) asymmetric junction structure (e.g., meta- or ortho-connected benzene rather than a para structure), and (c) minimal dephasing (implying low temperature) so as to maintain coherence between multiple pathways of conduction.

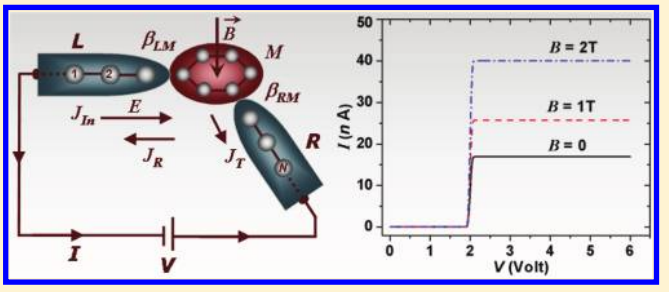

SECTION: Electron Transport, Optical and Electronic Devices, Hard Matter

Controlling electron transmission through molecular junctions that comprise molecular ring structures by magnetic fields is considered to be challenging because the required field strengths are believed to be unrealistically high, on the order of the Aharonov-Bohm period of $\sim 10^4$ Tesla for typical molecular rings.[1,2] Here we reconsider the possibility of controlling electrical conduction characteristics of molecular ring structures such as benzene, biphenyl, and anthracene by static uniform moderate magnetic fields. We follow the lead of refs 3−6, which indicate that large sensitivity to magnetic fields may be found in junctions where (a) electronic state degeneracy leads to interference that can be suitably tuned by the magnetic field and (b) weak molecule−metal coupling results in sharp transmission resonances. This implies that the behavior of such systems will strongly depend on junction geometry that determines the transmission pathways and on the effect of dephasing (decoherence) processes resulting from thermal motions in the junction.

In the present study, we analyze in detail the role of junction geometry and dephasing on the transport properties of molecular rings subject to external magnetic fields by means of a tight-binding (Hückel) Hamiltonian, focusing on the benzene structure as a model system. We show that weak lead-ring coupling, discussed in previous studies, is a necessary but insufficient condition to gain magnetic field control over the transport through the doubly degenerate energy levels of the benzene bridge. Asymmetric junction geometries accompanied by small dephasing rates are found to be essential to obtain experimentally detectable magnetic field effects in the $I-V$ characteristic of the molecular ring. In a subsequent expanded publication, we will show that most of our results are generic and are qualitatively similar in other, including more complex, ring structures as well as in continuum ring models. In fact, the underlying interference physics can be demonstrated in a simplified two-level model, where the two levels represent electronic wave functions with opposite angular momenta, whose degeneracy is split by coupling to the leads, an imposed magnetic field, or both.

In what follows, we first describe our model and theoretical approach, then present results of model calculations that describe (a) the magnetic field effect on the transmission probability and on the current voltage characteristics of simple molecular ring junctions; (b) the effect of structure, symmetry, and geometry on the dependence of junction transport properties on the applied magnetic field; and (c) the effect of dephasing processes on these behaviors. Possible experimental manifestations of our theoretical predictions are discussed in the summary section.

Our model junction comprises a ring molecule bridging two metal leads (L, R) through two chosen sites on the ring. The molecule is described by a tight-binding (Hückel) model with on-site energies α_M, nearest-neighbor interactions β_M, and interatomic distance of 0.139 nm. The metals can be modeled by any wide-band reservoir of a given electrochemical potential. For definiteness, they are modeled here as infinite 1-D tight-binding periodic arrays of atoms with on-site energies and nearest-neighbor coupling matrix elements α_K and β_K ($K \in L, R$), respectively. In the site representation, the corresponding tight binding Hamiltonian is given as

$$\hat{H} = \hat{H}_L + \hat{H}_R + \hat{H}_M + \hat{V}_{LM} + \hat{V}_{RM} \quad (1)$$

Received: June 26, 2011
Accepted: August 4, 2011

 © XXXX American Chemical Society

where

$$\hat{H}_K = \alpha_K \sum_{n \in K} |n\rangle\langle n| + \beta_K \sum_{n \in K} (|n\rangle\langle n+1| + |n+1\rangle\langle n|); \quad K = L, R, M \tag{2}$$

$$\hat{V}_{KM} = \beta_{KM}(|n\rangle\langle m| + |m\rangle\langle n|); \quad n \in K = L, R; \quad m \in M \tag{3}$$

where $\{|n\rangle\}$ is an orthogonal set of atomic orbitals centered at atomic sites n ($n \in K = L, R, M$). The indices $K = L$, R, and M correspond to the subspaces of the left (L), right (R), and molecule (M), respectively.

Models 1−3 are supplemented by an additional magnetic field $\vec{B}$ applied to the junction, so that the kinetic energy operator of an electron is modified according to $(2m_e)^{-1}\hat{\vec{p}}^2 \rightarrow (2m_e)^{-1}(\hat{p} + ((|e|\hat{\vec{A}})/c))^2$, where m_e and e are the electron mass and charge. We assume that the field is uniform, applied in the bridge region only and, for the planar ring-molecules considered, perpendicular to the molecular plane. In the standard London approximation,[7] one (a) represents this field as a vector potential in the symmetric gauge, $\vec{A}(\vec{r}) = {}^1/_2\vec{B} \times \vec{r}$, and (b) modifies the finite basis of field-free atomic orbitals $|n\rangle = \chi_n(\vec{r})$, where $\vec{r}$ is measured from the center of atom n so as to account for the phase difference between wave functions centered on different atomic sites

$$\chi_n(\vec{r}) \rightarrow \tilde{\chi}_n(\vec{r}) = \exp(-i(|e|/\hbar)\,\vec{A}_n \cdot \vec{r})\chi_n(\vec{r}) \tag{4}$$

where $\vec{A}_n = \vec{A}(\vec{r}_n)$. This leads to a tight binding (Hückel) Hamiltonian with coupling between atomic sites given by

$$\beta_{mn} = \int \mathrm{d}\vec{r}\; \chi_m^*(\vec{r}) V \chi_n(\vec{r}) \exp(-i(|e|/\hbar)(\vec{A}_n - \vec{A}_m)\cdot\vec{r})$$

For nearest neighbor interactions, $\vec{r}$ in the exponent is approximately replaced by $(\vec{r}_m + \vec{r}_n)/2$, leading to

$$\beta_M \rightarrow \beta_{mn} = \beta_M e^{i\theta_{mn}}; \quad n, m \in M \tag{5}$$

where

$$\theta_{mn} = -\frac{|e|}{\hbar}(\vec{A}_n - \vec{A}_m)\cdot\frac{\vec{r}_m + \vec{r}_n}{2} = \frac{|e|}{4\hbar}\,\vec{B} \times (\vec{r}_m - \vec{r}_n)\cdot(\vec{r}_m + \vec{r}_n) = \frac{|e|}{2\hbar}\vec{r}_m \times \vec{r}_n \cdot \vec{B} \tag{6}$$

and the molecular Hamiltonian is now given by

$$\hat{H}_M = \alpha_M \sum_{n \in M} |n\rangle\langle n| + \beta_M \sum_{n,m \in M} (e^{i\theta_{mn}}|m\rangle\langle n| + e^{-i\theta_{mn}}|n\rangle\langle m|) \tag{7}$$

Note that $|\vec{r}_m \times \vec{r}_n|$ is twice the area of the triangle spanned by the vectors, so $\theta_{mn} = 2\pi\delta\phi_B/\phi_0$, where $\delta\phi_B$ is the magnetic flux through the triangle spanned by the position vectors $(\vec{r}_n, \vec{r}_m)$ and $\phi_0 = h/|e|$ is the flux quantum.

To evaluate the transmission coefficient associated with this setup, we follow the scattering method used in refs 8 and 9 that yields the overall as well as the individual bond currents and, in its density matrix version, can be generalized to account (approximately) for dephasing processes. For any pair of nearest neighbor sites (m,n), this approach yields the bond transmission function $T_{nm}(E) = J_{nm}(E)/J_{in}(E)$, which is the ratio between the net bond current and the incoming current of electrons of energy, E. For a finite bias voltage, the net bond current between any two nearest neighbor sites in a two-terminal junction is obtained from the Landauer formula

$$I_{mn}(V) = \frac{e}{\pi\hbar}\int_{-\infty}^{\infty} T_{nm}(E)(f_L(E) - f_R(E))\,\mathrm{d}E \tag{8}$$

where $f_K(E)$ and μ_K ($K = L$, R) are the Fermi functions and chemical potentials of the left and right leads, respectively.

Two different procedures are used to model dephasing effects. In one, we introduce a damping rate η to the nondiagonal density matrix elements in the site representation. Alternatively, we use the Buttiker probe method,[10] where the dephasing rate at site j of the molecule is determined by its coupling $\beta_{j,J}$ to an external thermal electron reservoir, J, with chemical potential set such that no net current flows through the corresponding contact.

Next, consider the conduction properties of this model junction with and without an imposed magnetic field. As discussed above, current conduction through ring structures is inherently associated with interfering transmission pathways[11] that may be conveniently described in terms of degenerate eigenstates of the isolated ring. The corresponding degenerate states can be represented in terms of rotating, clockwise, and counter-clockwise Bloch states on the ring. Indeed, it is the tuning of the relative phases of these states by an external magnetic field that potentially provides control of the ring transmission properties. This implies several important aspects of the resulting behavior: First, transport will be affected by interference (and consequently most amenable to magnetic field control) in energy regimes dominated by such degenerate states. Second, strong interference effects and large sensitivity to magnetic field are expected when these states are associated with sharp transmission resonances, that is, for sufficiently weak metal-molecule coupling. Third, the symmetry of a given junction geometry strongly affects the interference pattern and hence dictates the transport properties. Fourth, these phenomena will be strongly influenced by dephasing processes.

The results presented below show several manifestations of these effects. In these calculations, the molecular junction is emulated by the tight binding (Huckel) molecular Hamiltonian and 1-D tight binding leads as presented above. For the latter, we take zero on-site energies, that is, α_K ($K \in L, R$) = 0, and nearest-neighbor coupling, $\beta_L = \beta_R = 6$ eV, that corresponds to a metallic band of width 24 eV. The zero bias Fermi energies of these contacts are set to $E_F = 0$. Unless otherwise stated, we have taken the leads temperature to be zero and assumed that the potential bias falls symmetrically on the metal−molecule interfaces, that is $\mu_L = E_F + \mathrm{eV}/2$ and $\mu_R = E_F - \mathrm{eV}/2$. For the molecular structure, we take α_M=−1.5 eV and β_M= 2.5 eV for all nearest-neighbor atom pairs. For free benzene molecules, the highest occupied molecular orbitals (HOMOs) and the lowest unoccupied molecular orbitals (LUMOs) constitute pairs of doubly degenerate orbitals, which, with our choice of molecular parameters and energy origin, are positioned at $\alpha_M - \beta_M = -4$ eV and $\alpha_M + \beta_M = 1$ eV, respectively. Upon connecting to the metal leads, these levels get broadened, and more importantly their

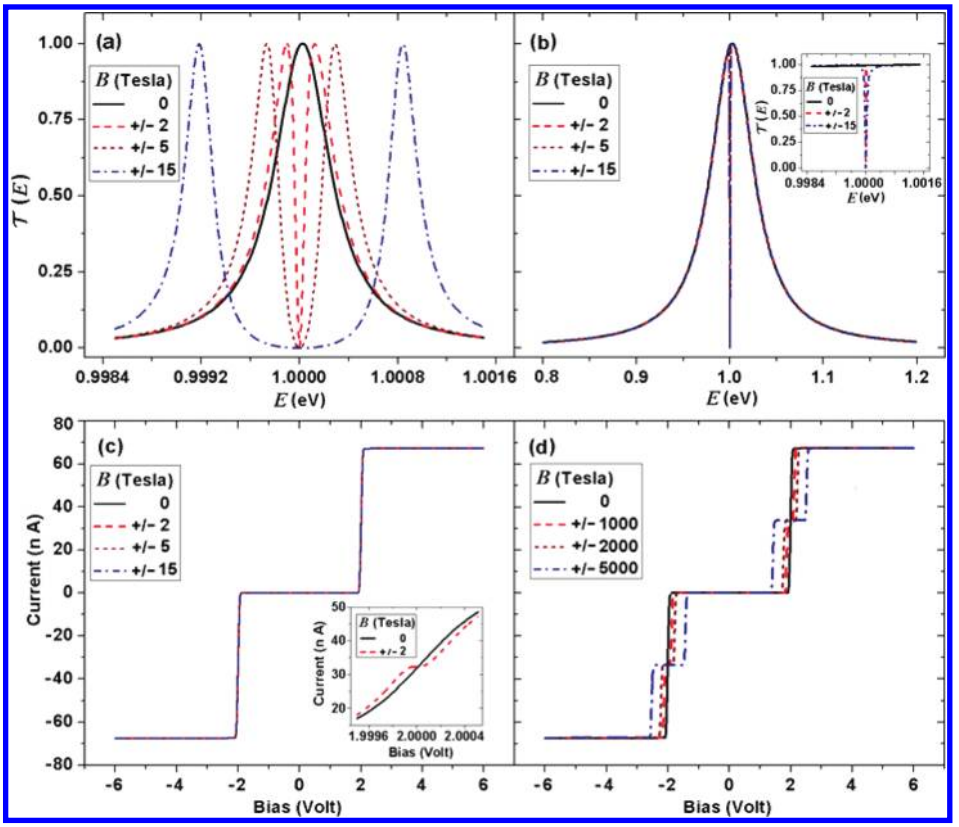

Figure 1. Transmission probability $\mathcal{T}(E)$ (a,b) and the $I-V$ characteristics (c,d) of a junction comprising para-connected benzene coupled to the leads with coupling element 0.05 (a,c,d) and 0.5 eV (b; the inset shows a close-up on the dip obtained at finite B) evaluated for different magnetic field strengths B normal to the ring. In the main panel of part c, the results obtained for different magnetic fields for the para system are essentially indistinguishable from each other. The inset in this part shows a close-up on the V = 2 V neighborhood that shows the consequence of the split degeneracy in the para-connected junction. Part d shows the magnetic field effect for unrealistically large field intensities.

degeneracy splits. For sufficiently weak metal−molecule coupling, β_{MK} (K = L, R), these split levels constitute sharp transmission resonances at the corresponding energies. When dephasing is considered via the Büttiker probe methods, we describe the probe by the same tight-binding metal model, eq 2, and the same energetic parameters (site energy and intersite coupling) as our source and drain leads. We use a single-parameter β_{BM} for all couplings of molecular sites to such probes. Similarly, when dephasing is considered using the density matrix method, we use a single parameter η for the damping of the nondiagonal elements of the molecular density matrix. We will see below that in addition to the junction symmetry, the molecule-lead coupling and the dephasing rate are the most important system parameters that determine the sensitivity of its transport behavior to an external magnetic field.

In several recent publications, we and others have studied the circular currents that can be induced on such molecular rings in a biased junction.[12] At issue now is the question of whether transport through such molecular rings can be affected by imposing an external magnetic field. Interestingly, previous studies[1,2] suggest that whereas the transmission $\mathcal{T}(E)$ may be affected by an external magnetic field, the integrated transmission, which yields the current−voltage characteristics, is not. Similar conclusions may be drawn from Figure 1, which shows the transmission probability $\mathcal{T}(E)$ and the $I-V$ characteristic of para-connected benzene molecule. $\mathcal{T}(E)$ is shown in Figure 1a, which focuses on the doubly degenerate (in the free molecule) molecular resonance at 1 eV. When the molecule-lead coupling is weak enough (here taken to be β_{KM} = 0.05 eV), the resonance splitting affected by a magnetic field is clearly seen. This very small splitting is completely erased for larger molecule-leads coupling, as seen in Figure 1b, where β_{KM} = 0.5 eV. Furthermore, it is found that the area under the $\mathcal{T}(E)$ curve does not change with B, so the integral over any Fermi window that encompasses this spectral structure to give the $I-V$ characteristics, does not depend on the imposed magnetic field for realistic field intensities, as seen in Figure 1c. Note that for symmetric voltage distribution in the junction, the molecular resonance at 1 eV is manifested by current steps at $V = \pm 2$ V (Figure 1c) that are seen to be insensitive to B. Only by zooming into the current step region (inset in Figure 1c) does one find a small shoulder resulting from the level splitting at a finite magnetic field value. This, however, requires bias and gate voltage precision smaller than the level splitting and very low temperatures. It should be noted that another regime of field dependence takes place at very high fields (Figure 1d), where shifting of energy levels causes other levels to appear within the Fermi window between μ_L and μ_R. For molecular scale loops, however, this happens at field intensities that are unrealistically large (∼1000T) and therefore will not be further discussed. Note that this is the regime (in terms of ϕ_B/ϕ_0) where the Aharonov-Bohm effect is observed in mesoscopic rings.

Observations such as those discussed above, together with the obvious fact that the magnetic field associated with the

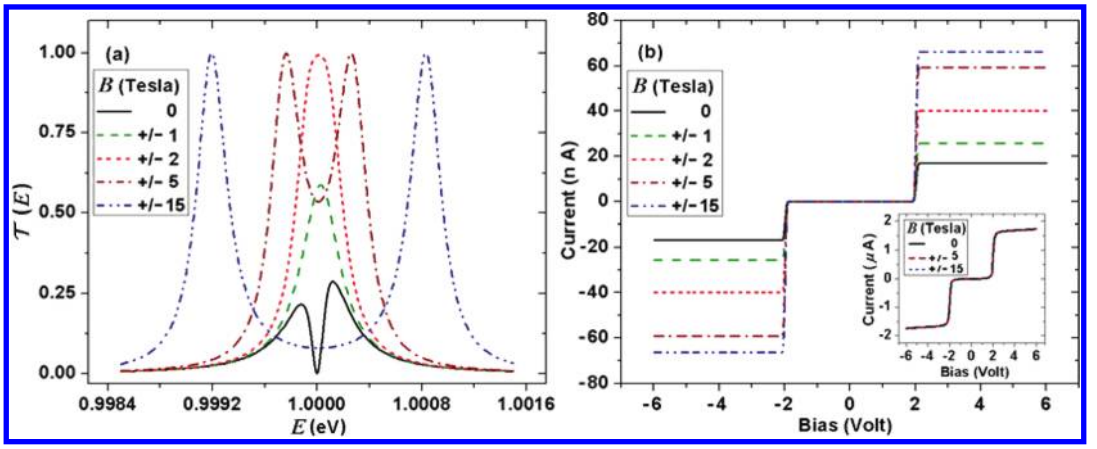

Figure 2. (a) Transmission probability $\mathscr{T}(E)$ around E = 1 eV through a junction comprising meta-connected benzene coupled to the leads with coupling matrix element 0.05 eV, evaluated for different magnetic field strengths B normal to the plane of the ring. (b) Current−voltage behavior of this junction for the different magnetic field intensities. The inset in part b shows the same current−voltage plots for molecule-leads coupling 0.5 eV. Here sensitivity to the magnetic field disappeared, and results for different values of B overlap. Results for the ortho-connected molecule are qualitatively similar to those shown here for the meta configuration.

Aharonov-Bohm period ϕ_0 is unrealistically large for small molecular loops, are presumably the source of a general belief that magnetic field effects cannot be observed in molecular conduction junctions. However, a strikingly different behavior is found in junctions comprising weakly coupled meta- and ortho-connected ring molecules. Figure 2a, an analog of Figure 1a, shows the transmission probability of a meta-connected benzene junction under an external magnetic field perpendicular to the molecular plane, again with molecular lead coupling 0.05 eV. First note that the asymmetric coupling to the leads results in degeneracy split even in the absence of external magnetic field. As B is increased, this splitting reduces up to a certain magnetic field intensity (here at about ±2 T with other values observed for different molecule-lead couplings), where it vanishes (level crossing), engendering constructive interference at this field value. This can be understood as phase adjustment of the interfering electron waves by the field, causing them to interfere constructively until full resonant transmission is reached. Interestingly, in this regime of magnetic field strengths, not only the splitting but also the area under the transmission function is field-dependent. Initially, as constructive interference builds up and the transmission peaks merge, the total area under the transmittance peaks increases with increasing magnetic field. Consequently, in the corresponding $I-V$ plots (Figure 2b), the current steps are found to be very sensitive to the imposed magnetic field intensity. As the field is further increased, the transmittance peaks split again until they become fully separated. At this point, the total area under the transmittance peak becomes insensitive to the intensity of the external field, and only the peak position changes. Finally, as discussed above, for unrealistically large magnetic fields, other energy levels enter the Fermi integration window, and the $I-V$ curve changes accordingly.

As can be seen in the inset of Figure 2, when the lead-molecule coupling is high such that the conduction resonance is broadened, the $I-V$ curve becomes insensitive to the intensity of the applied magnetic field, even in the asymmetric junction configuration (ortho- or meta-connected benzene ring).

As we will show in a subsequent expanded publication, the observations obtained for the benzene molecule regarding the sensitivity of the $I-V$ behavior to relatively weak external magnetic fields represent generic phenomena that appear in many ring molecular structures characterized by weak molecule-lead coupling. In particular, the results shown in Figure 2b suggest that in asymmetrically connected junctions the magnetic field dependence of the $I-V$ curve should be experimentally observable in the low lead-ring coupling regime. Details of this behavior depend on the electronic structure of the molecule and on the junction geometry. Keeping in mind that this behavior originates from interference between transmission pathways, we next turn to consider the effect of dephasing processes on these findings.

Dephasing effects in nanojunction transport are often discussed using the Büttiker probe method.[10] Because this phenomenological method is based on a rather artificial process of replacing coherently transmitted electrons by electrons with an indeterminate phase, we chose to compare such results with those obtained from a density matrix approach[8,9,12] often used in spectroscopy, where phenomenological damping is imposed on the nondiagonal elements of the junction density matrix in the spirit of the Bloch or Redfield theories of relaxation in a multilevel system. In the former approach, the dephasing rate is determined by the molecule-probe coupling, here denoted β_{BM}. In the latter, the process is governed by the coherence relaxation rate η. In both approaches, it is possible to affect dephasing locally, that is, at any given site of the tight-binding representation of the molecular ring.

Figure 3 compares results from these calculations in the absence of a magnetic field. Here dephasing is applied to all sites of the molecular (benzene) ring, and the transmission coefficient is plotted against electron energy for the para- and meta-connected benzene molecules (results for the ortho case are similar to those of the meta structure) for different values of the dephasing parameters. We note in passing that our calculations using the Büttiker probe method are practically identical to those obtained by Dey et al.[13] when the same junction parameters are used. On this level of presentation, the main effect of dephasing is seen to be broadening of the transmission peaks.

The two different phenomenological models of dephasing used here give qualitatively similar results. An immediate

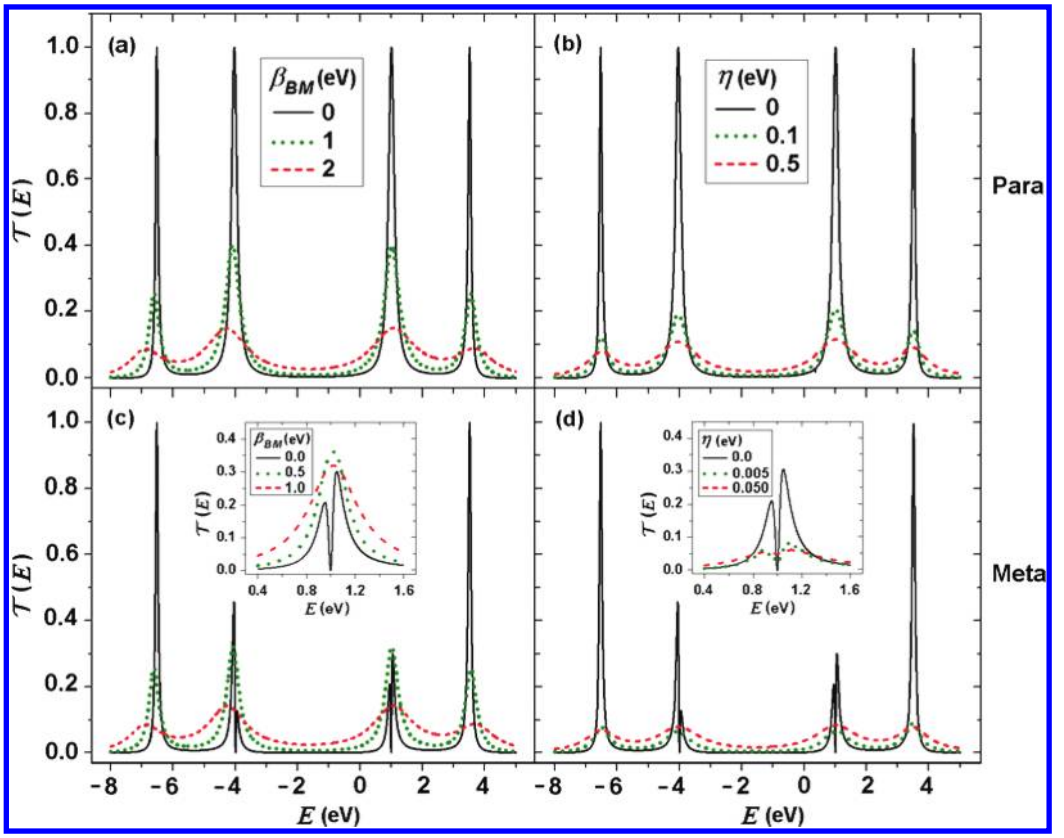

Figure 3. Transmission probability as a function of energy in the presence of dephasing: Top and bottom figures correspond to para- and meta-connected benzene molecules, with molecule-leads coupling taken 1 eV. Left: Results obtained using the Büttiker probe model with the indicated coupling parameter β_{BM}. Right: results obtained by the density-matrix calculation with the indicated dephasing rate η. The inset in the lower (meta) panels show a close-up in the resonance at 1 eV.

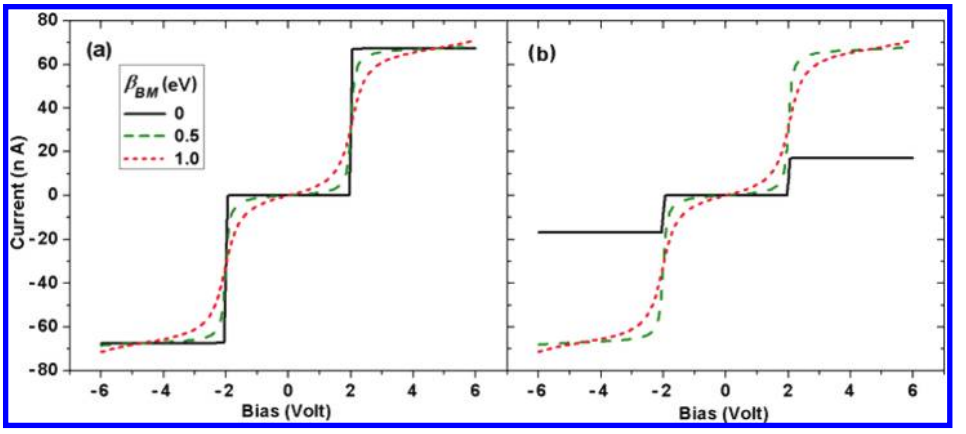

Figure 4. Current−voltage behavior in (a) para- and (b) meta-connected benzene for different dephasing strengths (imposed by the Büttiker probe method) near the molecular resonance at 1 eV (voltage bias 2 V), with molecule-lead coupling β_{KM} = 0.05 eV. Similar results are obtained using the density matrix approach.

consequence of dephasing is broadening accompanied by elimination of interference effect, as seen in the insets of Figure 3c,d. This in fact affects the conductance in an essential way, particularly in the weak molecule-lead coupling case. Figure 4 shows the $I-V$ behavior associated with the molecular resonance at 1 eV for molecule-lead coupling 0.05 eV. In the para-connected bridge, the two ring arms are equal in length; therefore, at zero magnetic field, constructive interference occurs and the transmission probability peaks. As dephasing is introduced, the constructive interference is destroyed; therefore, beyond the onset of conduction at V = 2 V, the current is reduced. For the meta-connected molecule, the zero-field interference is destructive; therefore, the introduction of dephasing results in an increase of the current. Implementing dephasing by the density matrix method gives qualitatively similar results.

Finally, as seen in Figure 5, the destruction of coherence also has a drastic effect on the response of conduction to magnetic

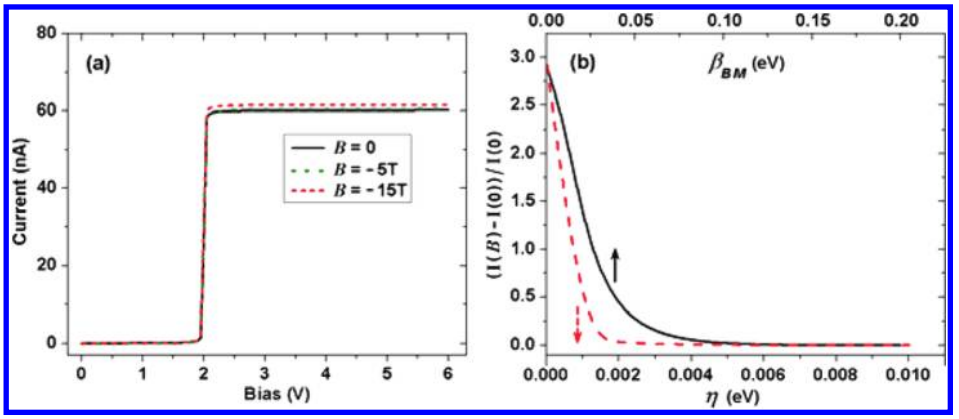

Figure 5. (a) Magnetic field dependence of the current near the 2 V step (associated with the transmission resonance at $E = 1$ eV; analog of Figure 2b) calculated for a meta-connected junction with molecule-lead coupling of 0.05 eV with dephasing implemented by the Büttiker probe method ($\beta_{BM} = 0.1$ eV); $B = 0$, -5, and -15 T. (b) Same magnetic field dependence expressed by the ratio $[I(B) - I(0)]/I(0)$ plotted, respectively, against the dephasing parameters β_{BM} (Büttiker probe method; solid-black curve) and η (density matrix method; dashed red curve) for $B = -15$T. In (a) the -5 T curve overlaps with that for 0 T.

field. The large magnetic field effect on the conduction properties of asymmetrically connected benzene molecules seen in Figure 2 is quickly erased with increasing dephasing. This implies that the field effect seen in Figure 2 can be observed only under conditions of slow dephasing. We have verified (not shown) that this effect arises from the dynamic destruction of phase and is not reproduced merely by raising the electronic temperature of the leads.

The requirement for small dephasing is inherent in all experiments trying to observe interference phenomena in molecular junctions and implies the need to work at relatively low temperatures. A shortcoming of the Buttiker-probe procedure is that it does not relate directly to physical dephasing processes and thus does not allow for a quantitative estimate of the conditions under which dephasing eliminates the coherent effects discussed above. However, the equivalent analysis in terms of the coherence damping rate η provides a reasonable estimate: For the realistic molecular parameters chosen in our calculations, Figure 5b shows that magnetic field effects are eliminated when dephasing rates exceed 0.001 to 0.002 eV, implying dephasing times on the order of 1 ps. Recent observations of electronic coherence persisting on such time scales even at room temperatures[14] suggest that such effects may be observable. From this observation, we can also infer that the magnetic field effect will also be sensitive to static perturbations of this order. Such perturbations may be caused, for example, by asymmetric coupling of the molecule to the electrodes, leading to an asymmetric potential drop across the molecule−electrode junctions. To check the sensitivity of the discussed coherent effects toward such perturbations, we have performed calculations showing that the magnetic field dependence of the $I-V$ characteristics of the asymmetric junctions toward the external magnetic field is insensitive to the choice of voltage division factors (the way the voltage bias is distributed between the two molecule-electrode contacts). Furthermore, we have performed calculations with modified molecular onsite energies simulating the electric field drop across the molecular junction. The results of these calculations indicate that static variations of the onsite energies up to 0.01 eV do influence the magnetic field effect but do not eliminate them.

To summarize, in this Letter we have discussed conditions under which magnetic fields can affect the electronic transport in molecular conduction junctions comprising molecular rings. We have found that strong magnetic field effects can be seen under the following conditions: (a) The molecular resonance associated with the conduction is at least doubly degenerate and associated with scattering electronic states of opposite angular momentum, as is often the case in molecular ring structures; (b) the molecule-lead coupling is weak, implying relatively distinct conduction resonances; (c) the molecule is coupled to the leads in an asymmetric structure; and (d) dephasing is weak (implying low temperature), so as to maintain coherence between multiple pathways of conduction.

It should be emphasized that the condition for weak molecule-lead coupling does not imply weak molecule-lead bonding, only that the states associated with the resonances that involve multiple pathways through the ring (or counter propagating wave functions in the ring) are weakly coupled to the metal electrodes. This can be achieved, for instance, by connecting a molecular ring to the leads via saturated alkane chains.

The generic nature of the effects discussed above (which, as pointed out before, can be reproduced in a model comprising a free particle traversing a circular ring junction as well as in a reduced two-level model) suggests that they will persist also in more sophisticated treatments. Moreover, despite the observed sensitivity to dephasing processes and static perturbations, our calculations indicate that they may still be amenable to experimental observation.

■ ACKNOWLEDGMENT

The research of A.N. is supported by the Israel Science Foundation, the Israel-US Binational Science Foundation, the European Science Council (FP7/ERC grant no. 226628), and the Israel − Niedersachsen Research Fund. O.H. acknowledges the support of the Israel Science Foundation under grant no. 1313/08, the support of the Center for Nanoscience and Nanotechnology at Tel-Aviv University, and the Lise Meitner-Minerva Center for Computational Quantum Chemistry. D.R. Acknowledges a Fellowship received from the Tel Aviv University Nanotechnology Center.

■ REFERENCES

(1) Walczak, K. The Role of Quantum Interference in Determining Transport Properties of Molecular Bridges. *Cent. Eur. J. Chem.* **2004**, *2*, 524–533.

(2) Maiti, S. K. Quantum Transport through Organic Molecules. *Chem. Phys.* **2007**, *331*, 254–260.
(3) Hod, O.; Baer, R.; Rabani, E. Feasible Nanometric Magnetoresistance Devices. *J. Chem. Phys. B* **2004**, *108*, 14807–14810.
(4) Hod, O.; Baer, R.; Rabani, E. A Parallel Electromagnetic Molecular Logic Gate. *J. Am. Chem. Soc.* **2005**, *127*, 1648–1649.
(5) Hod, O.; Rabani, E.; Baer, R. Magnetoresistance of Nanoscale Molecular Devices. *Acc. Chem. Res.* **2006**, *39*, 109–117.
(6) Hod, O.; Baer, R.; Rabani, E. Magnetoresistance of Nanoscale Molecular Devices Based on Aharonov−Bohm Interferometry. *J. Phys: Condens. Mat.* **2008**, *20*, 383201/1–383201/32.
(7) London, F. Théorie Quantique des Courants Interatomiques dans les Combinaisons Aromatiques (Quantum Theory of Interatomic Currents in Aromatic Combinations). *J. Phys. Radium* **1937**, *8*, 397–409.
(8) Ben-Moshe, V.; Nitzan, A.; Skourtis, S. S.; Beratan, D. Steady State Theory of Current Transfer. *J. Phys. Chem. C* **2010**, *114*, 8005–8013.
(9) Ben-Moshe, V.; Rai, D.; Nitzan, A.; Skourtis, S. S. Steady State Current Transfer and Scattering Theory. *J. Chem. Phys.* **2010**, *133*, 054105/1–054105/9.
(10) Buttiker, M. Role of Quantum Coherence in Series Resistors. *Phys. Rev. B* **1986**, *33*, 3020–3026.
(11) Hansen, T.; Solomon, G. C.; Andrews, D. Q.; Ratner, M. A. Interfering Pathways in Benzene: An Analytical Treatment. *J. Chem. Phys.* **2009**, *131*, 194704/1–194704/12.
(12) Rai, D.; Hod, O.; Nitzan, A. Circular Currents in Molecular Wires. *J. Phys. Chem. C* **2010**, *114*, 20583–20594 and references therein.
(13) Dey, M.; Maiti, S. K.; Karmakar, S. N. Effect of Dephasing on Electron Transport in a Molecular Wire: Green's Function Approach. *Org. Electron.* **2011**, *12*, 1017–1024.
(14) Ishizaki, A.; Calhoun, T. R.; Schlau-Cohen, G. S.; Fleming, G. R. Quantum Coherence and its Interplay with Protein Environments in Photosynthetic Electronic Energy Transfer. *Phys. Chem. Chem. Phys.* **2010**, *12*, 7319–7337.